

Thermal reversibility in electrical characteristics of ultraviolet/ozone-treated graphene

Yana Mulyana, Masahiro Horita, Yasuaki Ishikawa, Yukiharu Uraoka, and Shinji Koh

Citation: *Applied Physics Letters* **103**, 063107 (2013); doi: 10.1063/1.4818329

View online: <http://dx.doi.org/10.1063/1.4818329>

View Table of Contents: <http://scitation.aip.org/content/aip/journal/apl/103/6?ver=pdfcov>

Published by the [AIP Publishing](#)

Articles you may be interested in

[Highly reproducible and reliable metal/graphene contact by ultraviolet-ozone treatment](#)

J. Appl. Phys. **115**, 114304 (2014); 10.1063/1.4868897

[Electrical properties of TiN on gallium nitride grown using different deposition conditions and annealing](#)

J. Vac. Sci. Technol. A **32**, 02B116 (2014); 10.1116/1.4862084

[Extreme ultraviolet induced defects on few-layer graphene](#)

J. Appl. Phys. **114**, 044313 (2013); 10.1063/1.4817082

[Experimental investigation of electron transport properties of gallium nitride nanowires](#)

J. Appl. Phys. **104**, 024302 (2008); 10.1063/1.2952035

[Environmental and thermal aging of Au/Ni/p-GaN ohmic contacts annealed in air](#)

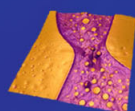
J. Appl. Phys. **91**, 3711 (2002); 10.1063/1.1448885

Asylum Research Atomic Force Microscopes

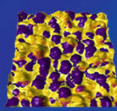
Unmatched Performance, Versatility and Support



The Business of Science®

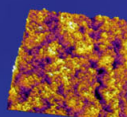


Modulus of Polymers
& Advanced Materials



Piezoelectrics
& Ferroelectrics

Coating Uniformity
& Roughness



Nanoscale Conductivity
& Permittivity Mapping



+1 (805) 696-6466
sales@AsylumResearch.com
www.AsylumResearch.com

Thermal reversibility in electrical characteristics of ultraviolet/ozone-treated graphene

Yana Mulyana,¹ Masahiro Horita,¹ Yasuaki Ishikawa,¹ Yukiharu Uraoka,¹ and Shinji Koh^{1,2,a)}

¹Graduate School of Materials Science, Nara Institute of Science and Technology, 8916-5 Takayama, Ikoma, Nara 630-0192, Japan

²Department of Electrical Engineering and Electronics, Aoyama Gakuin University, Sagamihara, Kanagawa 252-5258, Japan

(Received 16 April 2013; accepted 27 July 2013; published online 9 August 2013)

Changes in electrical properties of a bilayer graphene-based field-effect transistor (G-FET) after being oxidized through ultraviolet (UV)/ozone (O₃) treatment are presented. A decrease in conductivity and carrier mobility was observed after oxidation. However, electrical properties recovered after annealing oxidized G-FET with H₂/Ar, indicating that oxidation with UV/O₃ treatment was thermally reversible. Raman spectroscopy was conducted to verify that no defects were introduced after oxidation. The existence of chemical bonds between oxygen and graphene was confirmed from the X-ray photoelectron spectroscopy. Moreover, we found that graphene's sheet resistance increased after oxidation. Nevertheless, contact resistivity at graphene-Au/TiN electrode interface remained unchanged. © 2013 AIP Publishing LLC. [<http://dx.doi.org/10.1063/1.4818329>]

Graphene holds great promise to be applied in next-generation electronics because of its exceptional physical and electronic properties, i.e., high field-effect charge mobility as high as 15 000 cm²/Vs at room temperature.¹⁻³ Significant research activities in the field of chemical functionalization of graphene have been actively pursued in efforts to explore and modify its properties.^{4,5} An alternative approach has recently been reported for oxidizing graphene using reactive atomic oxygen in an ultrahigh vacuum to form chemically homogeneous and thermally reversible graphene oxide (GO).⁶ Indeed, the chemical functionalization of graphene can be a way of improving the performance of graphene-based devices,⁷⁻⁹ and ultraviolet (UV)/ozone (O₃) treatment is considered to be a promising route to enhance the weak chemical reactivity of graphitic structures.¹⁰⁻¹² Nevertheless, changes in the electrical properties of graphene after being oxidized are still seldom studied and remain to be fully investigated.

Changes in electrical properties of bilayer graphene, such as its conductivity and carrier mobility, after being oxidized through UV/O₃ treatment, and the mechanism are presented. The electrical properties of graphene were evaluated by measuring the current-gate voltage (I_d-V_g) characteristics of graphene-based field-effect transistors (G-FETs). The thermal reversibility of the oxidation process was also investigated by conducting H₂/Ar anneal treatment. Raman spectroscopy measurements were carried out after each process of oxidation and reduction to find whether the processes introduced any significant defects into graphene lattice. The existence of chemical bonds between oxygen and carbon atoms (C-O) in graphene layer was proven by performing X-ray Photoelectron Spectroscopy (XPS) measurements of chemically vapor deposited (CVD)-graphene. Finally, graphene's sheet resistance and contact resistance at graphene-electrode interface were examined using the transfer length method (TLM).¹³

A bilayer G-FET that was 10 μm long and 3 μm wide was used in this experiment. The bilayer graphene was

transferred onto a 100-nm SiO₂/p⁺-Si substrate using the micromechanical cleavage of Kish graphite.¹⁴ The number of layers was determined by optical contrast and Raman spectroscopy.¹⁵ The G-FET was fabricated by using photolithography to print source/drain patterns onto both ends of the graphene layer and depositing Au/TiN (100/50 nm) metals with a process of electron beam vapor deposition followed by a lift-off process in acetone for 10 min. A bottom-gate was constructed by attaching a Cu plate onto the bottom of SiO₂/Si substrate using silver paste, after lower SiO₂ layer of the substrate was removed with buffered hydrofluoric acid solution. Electrical characterization was carried out under vacuum conditions of 4.6 × 10⁻⁵ Pa using a nano-probing microscopy (Hitachi NE4000).

The G-FET was oxidized with UV/O₃ treatment and then reduced by H₂/Ar annealing. The UV/O₃ treatment was performed using a UV/O₃ cleaning system where the G-FET was treated for 3 min, and the hot plate temperature was set to 25 °C. Oxygen gasses in this equipment were channeled into the chamber at a flow rate of 500 cm³/min, and two types of UV light with wavelengths of 184.9 nm and 253.7 nm were simultaneously produced from a low pressure mercury lamp so that reactive oxygen atoms were eventually produced inside the chamber. The H₂/Ar anneal treatments were undertaken in a tube annealing furnace in which the G-FET was annealed at a temperature of 300 °C for 2 h, and H₂ and Ar gasses were simultaneously channeled into the tube furnace at a flow rate of 200 cm³/min. Actively reducing gas such as H₂ was introduced to create a reducing atmosphere, and inert gas such as Ar was introduced to prevent reactions between the samples and oxygen. Raman spectroscopy measurements were carried out after each process to determine whether the oxidation and reduction processes had introduced any significant defects into graphene lattice using ~1 mW of 514.5 nm light from an Ar laser.^{16,17} The beam's spot size was ~1 μm. Another experiment in which XPS spectra of oxidized CVD-graphene were measured was conducted to investigate whether oxygen atoms chemically

^{a)}koh@ee.aoyama.ac.jp

TABLE I. Changes in G-FET characteristic.

Sequential order	Process	μ^a (cm ² /Vs)	$V_{G-\min}^b$ (V)	$I_{D-\min}^c$ (A)	I_G^d (A)
1	1 st annealing ^e	2500	13.2	25.8	10 ⁻¹²
2	1 st oxidation	2100	31.8	18.5	10 ⁻¹²
3	2 nd annealing ^f	2400	16.2	25.3	10 ⁻⁹
4	3 rd annealing ^e	3000	3.0	28.3	10 ⁻⁹
5	2 nd oxidation	2500	8.4	20.2	10 ⁻⁹
6	4 th annealing ^f	3000	-1.8	28.3	10 ⁻⁹

^a μ is carrier mobility.

^b $V_{G-\min}$ is back-voltage at minimum conductivity, i.e., Dirac point.

^c $I_{D-\min}$ is drain current at minimum conductivity.

^d I_G is maximum leakage current.

^eThis is performed for cleaning purpose.

^fThis is performed to reduce oxidized graphene.

reacted with carbon atoms of graphene. Since the area of graphene exfoliated with micromechanical cleavage was too small to be measured in the XPS spectrometer,¹⁴ CVD-graphene, which is graphene grown on Cu foil with CVD and has a relatively large area, was used in this experiment. The oxidized CVD-graphene was then annealed with H₂/Ar, and its XPS spectra were measured. The pass energy was 40 eV, and the anode HT (high tension) was 15 kV. The step energy resolution was ~20 meV. The contact resistance and sheet resistance of graphene before and after oxidation were determined using the TLM.¹³ Three-layered graphene with four Au/TiN-electrodes was used in these measurements. Results for the measurements of G-FET characteristics at each oxidation/reduction process and the results for XPS and Raman measurements are summarized in Tables I and II, respectively.

The XPS spectra of pristine CVD-graphene after oxidation and reduction are shown in Fig. 1, and the XPS peak concentrations at each process are summarized in Table II, where an additional peak emerged as a result of oxidation. This peak can be attributed to the C-O bond from its energy binding.¹⁸ This may be evident that reactive oxygen atoms chemically reacted with carbon atoms of graphene during UV/O₃ treatment to form epoxide groups, resulting in a GO layer. Other oxygen functional groups were not detected from this XPS measurement. The peak vanished after H₂/Ar annealing, indicating that C-O bonding had broken and CVD-graphene layer recovered to its pristine order as a result of reduction performed by H₂/Ar annealing.⁶

TABLE II. Changes in XPS and Raman spectroscopy features.

Sequential order	Process	Concentration ^a		
		C-C ^b (%)	C-O ^b (%)	D/G ^c (a.u.)
1	Pristine graphene ^d	100	0	0
2	After oxidation	81	19	0
3	After reduction	97	3	0

^aConcentration was quantified by C-C and C-O peak area.

^bBinding energy position is 284.8 eV for C-C and 286.4 eV for C-O.

^cThe degree of lattice defect was quantified by the area ratio of D band and G band in Raman spectroscopy.

^dCVD-graphene was used in XPS, and mechanically exfoliated graphene was used in Raman measurement.

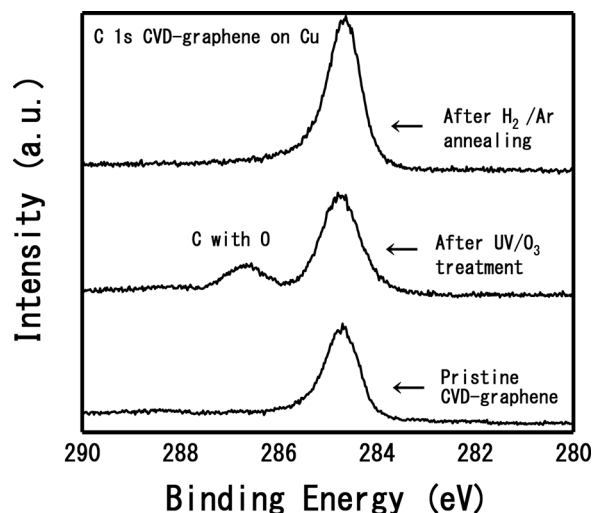


FIG. 1. C 1s XPS spectra of pristine CVD-graphene after being oxidized and then annealed.

The Hummers method is widely used for oxidizing graphene. Aggressive acidic treatments are used in this method, resulting in a chemically inhomogeneous surface with a range of oxygen functional groups, such as carboxylic, hydroxyl, and carbonyl groups, and structural defects that degrade the charge mobility and compromise its usability in high-performance devices.^{6,19} On the other hand, oxidation by UV/O₃ treatment produced reversible and homogeneous GO with only functional group of epoxide without any structural defects. Several ways of reducing GO have been reported, including reduction by excimer laser radiation. Although the high fluence laser radiation fragmented graphene sheets into smaller flakes, it can be utilized as laser patterning processes.¹⁹ Reduction of GO through H₂/Ar annealing used in this study can still maintain graphene layer perfectly intact without any structural defects.

The G-FET's I_d - V_g characteristics after the first oxidation through UV/O₃ treatment are plotted in Fig. 2. Prior to that the G-FET was cleaned through H₂/Ar annealing. The

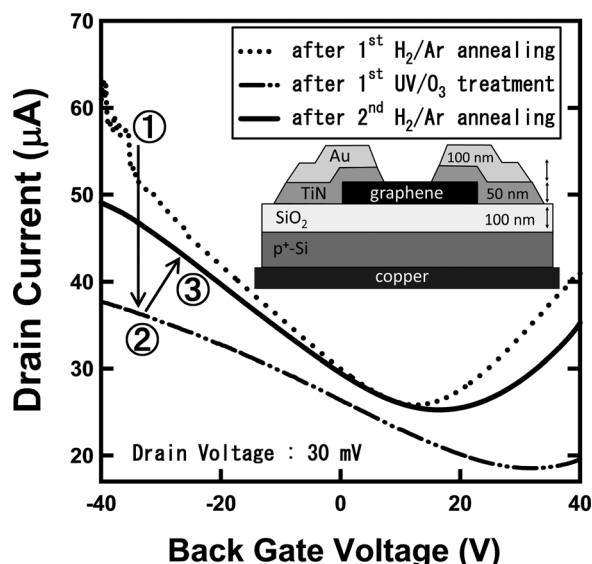


FIG. 2. Graphene-based FET's I_d - V_g characteristics after first oxidation and reduction process. Inset shows device structure.

ambipolar curve shifted downward after oxidation, from curve No. 1 to No. 2, suggesting decreased conductivity. The carrier mobility slightly decreased from 2500 to 2100 cm^2/Vs , indicated by the decreased curve slope. These values are comparable to the variations in the carrier mobility of bilayer graphene, ranged between 1500 and 4000 cm^2/Vs , reported by Novoselov *et al.*³ and Nagashio *et al.*¹⁵ A positive shift in the Dirac point can be observed and could be attributed to charged impurities that physically adhered to graphene surface during UV/O₃ treatment. It is probable that the impurities were negatively charged by considering that it was a positive shift. However, after annealing the oxidized G-FET with H₂/Ar, the ambipolar curve almost perfectly recovered to the state before oxidation, as indicated by curve No. 3. The carrier mobility recovered to 2400 cm^2/Vs , 96% of its previous level, and the minimum conductivity recovered to almost 100% of its previous level. This high (more than 90%) recovery of carrier mobility and minimum conductivity could be an assessment of thermally reversibility of oxidation through UV/O₃ treatment.

UV/O₃ treatment could cause reactive oxygen atoms to chemically react with carbon atoms in the graphene to form oxide groups by taking into account the results of XPS measurements of oxidized CVD-graphene.¹⁸ It appears that in this reaction a certain number of π electrons of graphene were used in the formation of C-O bond. On the other hand, during reductive H₂/Ar annealing, hydrogen reacted with chemically doped oxygen atoms to form H₂O, which were eventually exhausted and caused C-O bonds to break, leaving the π electrons unbound. In the formation of C-O bonds, as a result of oxidation, a number of π electrons were used in the chemical bonding and yet bound. This forced those π electrons to stop functioning as charge carriers, eventually causing a decline in the number of charge carriers. Since π electrons, which act as charge carriers, are responsible for electrical conductivity of graphene,² the decline in number of charge carriers resulting in the decreased conductivity. Therefore, oxidation caused a decrease in the number of charge carrier and hence in conductivity which was indicated by the downshift of ambipolar curve. Since not all of the π electrons were used in C-O bonds, the ambipolar characteristics of graphene can still be observed after oxidation. Nevertheless, subsequent reduction caused C-O bonds to break, leaving those π electrons unbound, and hence restored the number of charge carrier as well as ambipolar transfer characteristic to its pristine level.

It seems likely that after oxidation, the formation of C-O bond obstructed the path of charge carrier and hence increased carrier scattering in graphene. Since charge mobility is directly affected by various scattering, the increased scattering eventually suppressed the charge mobility of G-FET. Nonetheless, subsequent reduction caused C-O bonds to break, clearing the oxidized path of charge carrier, and hence recovered the charge mobility of G-FET to its pristine level, resulting in the recovery of the conductivity. The conductivity regaining in reduction of GO was reported by Kumar *et al.*, in which the increase in conductivity by two orders of magnitude was achieved upon reduction of GO through excimer laser irradiation.²⁰ They also reported the difference in

luminescence properties between GO and reduced GO besides the difference in conductivity.²¹

The G-FET's I_d - V_g characteristics after the second oxidation are plotted in Fig. 3. Prior to that, H₂/Ar annealing was repeated to clean the graphene's surface. As indicated by curve No. 1, the Dirac point was observed near zero back-gate voltage, suggesting that most charged impurities that physically adhered to graphene surface were cleaned. After the second oxidation, exactly like after the first one, the ambipolar curve shifted downward from curve No. 1 to No. 2, indicating decreased conductivity from 3000 to 2500 cm^2/Vs . Moreover, a positive shift in the Dirac point due to negatively charged impurities, similar to that found after the first oxidation, was observed. However, after keeping the device inside the vacuum chamber (4.6×10^{-5} Pa) for 24 h, the I_d - V_g curve horizontally shifted back to near zero back-gate voltage, from curve No. 2 to No. 3, indicating that the impurities were swept. The carrier mobility during this shifting remained at a level of 2500 cm^2/Vs .

It seems reasonable to assume that the impurities did not chemically react with carbon atoms of graphene and only physically adhered to the surface instead. If the impurities had chemically reacted with carbon atoms, this would have caused a decline in the number of charge carriers which decreases the conductivity. If that were the case, conductivity would have recovered, and vertical shift would have been observed, as the impurities vanished (from curve No. 2 to No. 3). Additionally, further studies are needed to identify the charged impurities and to determine details of their profiles. However, in the case of oxygen-doped graphene, oxygen atoms chemically reacted with carbon atoms, and the chemical bonds were stable. That may explain the fact that even after the oxygen-doped G-FET had been kept for more than 24 h inside the vacuum chamber, and the electrical conductivity did not recover by itself. Nonetheless, after the oxygen-doped G-FET had been annealed with H₂/Ar, the ambipolar curve almost perfectly recovered to its state before oxidation, as indicated by curve No. 4. The carrier mobility recovered to its previous level of 3000 cm^2/Vs . As

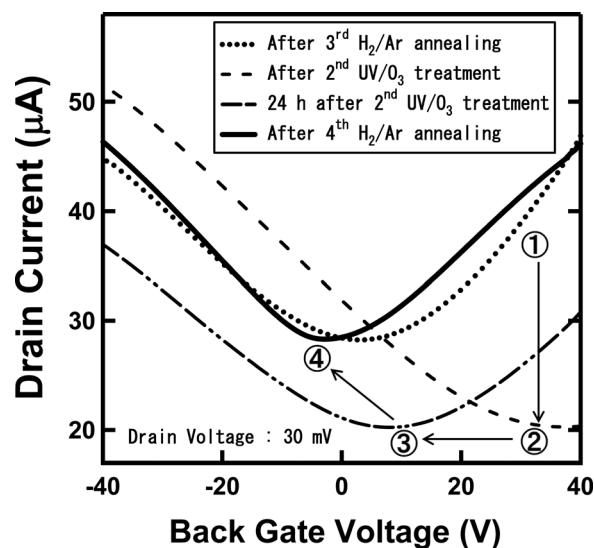


FIG. 3. Graphene-based FET's I_d - V_g characteristics after second oxidation and reduction process.

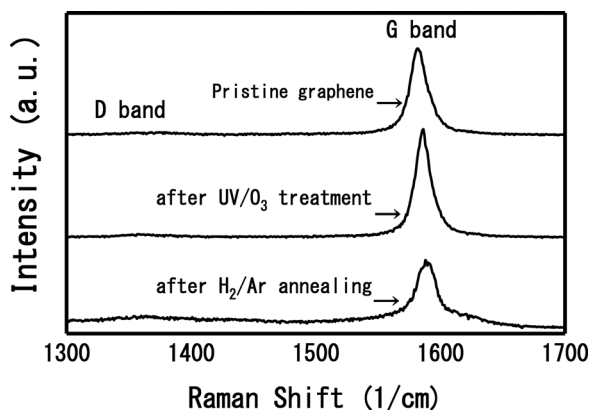


FIG. 4. Raman spectra of pristine graphene after being oxidized and then reduced.

summarized in Table I, the results may assess that oxidation through UV/O₃ treatment is thermally reversible, even after being done for multiple turns.

The Raman spectra of pristine graphene after oxidation and reduction are given in Fig. 4, where no distinct peaks in the D band feature of graphene can be observed as summarized in Table II. Since the D band is defect-induced band,^{16,17} this suggests that oxidation and reduction did not introduce any significant crystalline defects into graphene layers, even after annealing at 300 °C for 2 h. This could indicate that the decrease in conductivity was not caused by any defects in the structure of the graphene's crystal.

The contact resistance at the Au/TiN electrode-graphene interface before and after oxidation that was determined by TLM¹³ are plotted in Fig. 5. The contact resistance at metal-graphene interface (2R_c) before oxidation, 950 ± 170 Ω, or after oxidation, 1100 ± 120 Ω, did not differ significantly, indicating that oxidation did not increase the contact resistance. Nonetheless, the sheet resistance of graphene layer increased by ~20 Ω/μm after oxidation. This is comparable to the decreased conductivity of the G-FET after oxidation. Therefore, it is reasonable to conclude that changes in I_d-V_g characteristics are not caused by any change in the electrode-graphene interface but are instead related to the change in graphene's sheet resistance. It appears that contact resistivity at the electrode-graphene interface of Au/TiN, i.e., ~3500 Ωμm, is more versatile than that of conventional materials such as Au/Cr or Au/Ti, which both are approximately

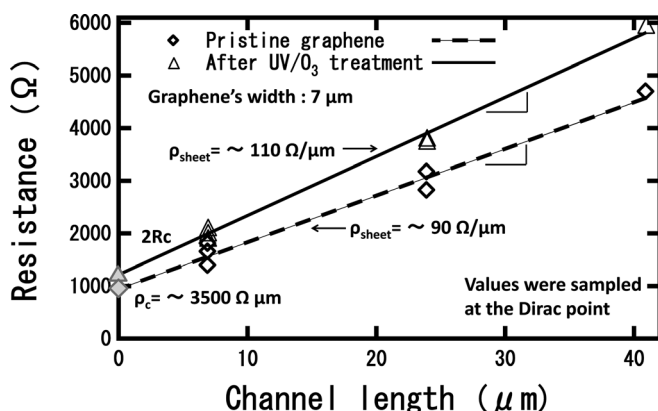


FIG. 5. Result of TLM measurement before and after oxidation process.

~10 000 Ωμm.²² In fact, contact resistivity at the electrode-graphene interface of Au/TiN could compete with that of Ni, which is ~2000 Ωμm.¹³ It seems that Au/TiN has something to offer considering that it is chemically inert and the adhesion with SiO₂ is excellent compared to that of Ni.²³

In summary, the changes in electrical properties of graphene after being oxidized through UV/ozone treatment were investigated. Reactive oxygen atoms chemically reacted with carbon atoms of graphene, which was confirmed from the XPS spectra. The conductivity of the graphene layer decreased as a result of oxidation. The electrical characteristics such as conductivity and carrier mobility recovered to the level before oxidation after annealing the oxidized graphene with H₂/Ar, suggesting that the oxidation of graphene with UV/ozone treatment is thermally reversible. The oxidation did not change the contact resistance at the Au/TiN electrode-graphene interface. The thermal reversibility of the redox reaction may suggest possibilities for applications to a nonvolatile memory and reconfigurable electric circuit.

This work was supported by the NAIST Cutting-Edge Research Project, the Green Photonics Research Project at NAIST by the Ministry of Education, Culture, Sports, Science and Technology of Japan (MEXT), and a Grant-in-Aid for Scientific Research (25600043) from the Japan Society for the Promotion of Science.

- ¹K. S. Novoselov, A. K. Geim, S. V. Morozov, D. Jiang, Y. Zhang, S. V. Dubonos, I. V. Grigorieva, and A. A. Firsov, *Science* **306**, 666 (2004).
- ²P. R. Wallace, *Phys. Rev.* **71**, 622 (1947).
- ³S. V. Morozov, K. S. Novoselov, M. I. Katsnelson, F. Schedin, D. C. Elias, J. A. Jaszczak, and A. K. Geim, *Phys. Rev. Lett.* **100**, 016602 (2008).
- ⁴A. H. C. Neto, F. Guinea, N. M. R. Peres, K. S. Novoselov, and A. K. Geim, *Rev. Mod. Phys.* **81**, 109 (2009).
- ⁵Y.-M. Lin, A. Valdes-Garcia, S.-J. Han, D. B. Farmer, I. Meric, Y. Sun, Y. Wu, C. Dimitrakopoulos, A. Grill, P. Avouris, and K. A. Jenkins, *Science* **332**, 1294 (2011).
- ⁶Md. Z. Hossain, J. E. Johns, K. H. Bevan, H. J. Karmel, Y. T. Liang, S. Yoshimoto, K. Mukai, T. Koitaya, J. Yoshinobu, M. Kawai, A. M. Lear, L. L. Kesmodel, S. L. Tait, and M. C. Hersam, *Nat. Chem.* **4**, 305 (2012).
- ⁷M. Y. Han, B. Oezylmaz, Y. Zhang, and P. Kim, *Phys. Rev. Lett.* **98**, 206805 (2007).
- ⁸M. Shan, Q. Xue, N. Jing, C. Ling, T. Zhang, Z. Yan, and J. Zheng, *Nanoscale* **4**, 5477 (2012).
- ⁹A. Hirsch, J. M. Englert, and F. Hauke, *Acc. Chem. Res.* **46**, 87 (2013).
- ¹⁰G. Lee, B. Lee, J. Kim, and K. Cho, *J. Phys. Chem. C* **113**, 14225 (2009).
- ¹¹S. Huh, J. Park, Y. S. Kim, K. S. Kim, B. H. Hong, and J.-M. Nam, *ACS Nano* **5**, 9799 (2011).
- ¹²S. Zhao, S. P. Surwade, Z. Li, and H. Liu, *Nanotechnology* **23**, 355703 (2012).
- ¹³K. Nagashio, T. Nishimura, K. Kita, and A. Toriumi, *Jpn. J. Appl. Phys.* **49**, 051304 (2010).
- ¹⁴P. Blake, E. W. Hill, A. H. C. Neto, K. S. Novoselov, D. Jiang, R. Yang, T. J. Booth, and A. K. Geim, *Appl. Phys. Lett.* **91**, 063124 (2007).
- ¹⁵K. Nagashio, T. Nishimura, K. Kita, and A. Toriumi, *Appl. Phys. Express* **2**, 025003 (2009).
- ¹⁶M. A. Pimenta, G. Dresselhaus, M. S. Dresselhaus, L. G. Cancado, A. Jorio, and R. Saito, *Phys. Chem. Chem. Phys.* **9**, 1276 (2007).
- ¹⁷D. Graf, F. Molitor, K. Ensslin, C. Stampfer, A. Jungen, C. Hierold, and L. Wirtz, *Nano Lett.* **7**, 238 (2007).
- ¹⁸N. Leconte, J. Moser, P. Ordejón, H. Tao, A. Lherbier, A. Bachtold, F. Alsina, C. M. S. Torres, J.-C. Charlier, and S. Roche, *ACS Nano* **4**, 4033 (2010).
- ¹⁹P. Kumar, B. Das, B. Chitara, K. S. Subrahmanyam, K. Gopalakrishnan, S. B. Krupanidhi, and C. N. R. Rao, *Macromol. Chem. Phys.* **213**, 1146 (2012).

²⁰P. Kumar, K. S. Subrahmanyam, and C. N. R. Rao, *Mater. Express* **1**, 252 (2011).

²¹K. S. Subrahmanyam, P. Kumar, A. Nag, and C. N. R. Rao, *Solid State Commun.* **150**, 1774 (2010).

²²K. Nagashio, T. Nishimura, K. Kita, and A. Toriumi, *Appl. Phys. Lett.* **97**, 143514 (2010).

²³C. N. Kirchner, K. H. Hallmeier, R. Szargan, T. Raschke, C. Radehaus, and G. Wittstock, *Electroanalysis* **19**, 1023 (2007).